Grating-mediated wave guiding and holographic solitons

Barak Freedman, Oren Cohen, Ofer Manela, and Mordechai Segev

Department of Physics and Solid State Institute, Technion, Haifa 32000, Israel

Jason W. Fleischer

Department of Electrical Engineering, Princeton University, Princeton, New Jersey 08544

Demetrios N. Christodoulides

School of Optics/CREOL, University of Central Florida, Orlando, Florida 32816-2700

Received November 15, 2004; accepted January 20, 2005

We describe experimental and theoretical results of research on a new type of waveguide, the so-called grating-mediated waveguide (GMW) recently reported by our group. This waveguide structure relies on Bragg diffractions from a 1D grating giving rise to wave guiding in the direction normal to the grating wave vector. The structure consists of a shallow 1D grating having a bell- or trough-shaped amplitude in the confinement direction. We provide the theoretical analysis of the underlying wave-guiding mechanism along with experimental evidence for both the bell- and the trough-shaped waveguides. We investigate the robustness of grating-mediated wave guiding and suggest more elaborate, 2D structures, such as a GMW superlattice and a grating-mediated ring waveguide. Finally we discuss the relation between grating-mediated wave guiding and holographic solitons, which are the beams that are self-trapped solely by virtue of their jointly induced grating.

OCIS codes: 190.5330, 090.7330, 230.7370.

1. INTRODUCTION

A great deal of research effort has been invested in the study of waveguides, since they serve as the backbone of modern communication.[1] Optical waveguides are widely used in modern optoelectronic systems, and new waveguide structures are being suggested constantly, such as chiral waveguides serving as filters for light pulses[2] and photonic-bandgap optical fibers.[3] To date, all optical waveguides can be classified into three generic categories. The most commonly used wave-guiding scheme relies on total internal reflection (TIR),[4,5] in which light propagates in a core region with a refractive index higher than that of the cladding, $n_{\mathrm{clad}} < n_{\mathrm{cor}}$. The second class of waveguides exploits the process of "Bragg reflection," and is sometimes called photonic-bandgap wave guiding.[6–8] In this scheme light is confined to a core region that is surrounded by stacks of alternating dielectric layers. The propagation constants of the guided modes reside in the forbidden gaps of the cladding's transmission spectrum; consequently, light is trapped as a result of Bragg reflection from the cladding regions. The third class of waveguides is based on the coupled-resonator-optical-waveguide system[9] in which wave guiding is achieved through weak coupling between adjacent high-Q optical microresonators.

We have recently proposed a new method for optical wave guiding: grating-mediated wave guiding[10] (GMW). GMW is driven by a shallow 1D grating with bell- or trough-shaped amplitude that is slowly varying in the direction normal to the grating wave vector. Wave guiding in this system occurs for a probe beam constructed of two Bragg-matched beams that are incident on the grating in an angularly symmetric fashion. These beams are simultaneously Bragg-reflected from the grating and are jointly guided in the direction normal to the grating wave vector. In our previous paper on this subject[10] we presented the basic underlying theory and an experimental proof of concept for the trough-shaped GMW. Here we describe a more comprehensive study of GMW, including experiments on both bell-shaped and trough-shaped GMWs and a theoretical study of the robustness and sensitivity to wave guiding conditions. In addition we propose more complex 2D GMW structures, such as a GMW superlattice and a grating-mediated ring waveguide; for completeness we repeat most of the results reported in Ref. 10.

As will be explained below GMW is considered generic and differs from the other three generic wave-guiding methods. This new technique can be implemented in wave systems beyond optics as well, such as matter waves in Bose–Einstein condensates and density waves in acoustics.

2. THEORETICAL BACKGROUND

The GMW mechanism is based on a shallow 1D grating that has a bell- or trough-shaped amplitude in the confinement direction. This bell–trough envelope changes the modulation depth of the grating, thus causing beams that

are Bragg-matched with the grating (beams at the edge of the Brillouin zone) to "feel" a different refractive index at different y levels. This in turn creates an effective lens that acts on the beams. Let us now discuss this GMW mechanism in more detail. For demonstration purposes let the refractive-index profile associated with such a planar GMW be given by

$$n(x,y) = n_0[1 + \varepsilon A(y)\cos(2\pi x/d)]. \quad (1)$$

This GMW consists of a shallow grating in x with periodicity d and amplitude $\epsilon A(y)$. In Eq. (1), $A(y)$ is a normalized profile ($0 \leqslant A(y) \leqslant 1$), and the small parameter ϵ ($0 < \epsilon \ll 1$) indicates the peak amplitude of the grating involved. The structure is uniform in the z direction, which is also the propagation direction of the waveguide. In this paper we will focus on two families of GMW corresponding to $A(y)$ having a bell shape [Fig. 1(a)] or a trough shape [Fig. 1(b)]. Note that in both cases the average index in every "layer" (cross section) in the y direction is equal to n_0, i.e., $\bar{n}(y) = \int_0^d n(x,y)\mathrm{d}x = n_0$.

We begin by giving a qualitative explanation of the basic mechanism underlying GMW. For this purpose we assume that the width of the grating amplitude is several times larger than the grating period and of course much larger than the wavelength. Within this limit the guided modes of these systems can be described by the modes of the 1D grating with their amplitudes slowly modulated (on a wavelength scale) in the y direction through the change in the grating amplitude. Figure 2(a) shows three gratings with different amplitudes corresponding to three different y planes (layers) of this structure. The dispersion curves in these layers, namely the propagation constant β versus the transverse momentum k_x, are shown in Fig. 2(b). The dispersion curves coincide everywhere except in the vicinity of the edge of the first Brillouin zone [shown in the magnified section of Fig. 2(b)], where a large amplitude ϵ yields a larger gap (outermost curves), and $\epsilon \to 0$ leads to a diminishingly small gap. The modes of shallow gratings are approximately plane waves $\exp(\pm ik_x x)$ or, equivalently, standing waves $\cos k_x x$ and $\sin k_x x$.[11] Because the grating is shallow, the curves for the different layers coincide, except near the edge of the Brillouin zone, that is, near $k_x = \pm\pi/d$, where the grating removes the degeneracy between the standing waves $\cos(\pi x/d)$ and $\sin(\pi x/d)$. In the vicinity of this region the wave with the $\cos(\pi x/d)$ dependence is more concentrated in the higher-index regions, whereas the $\sin(\pi x/d)$ wave is more concentrated in the lower-index regions. Hence the propagation constant (or equivalently the effective refractive index $n_{eff} = \beta/k_0$) of the cosine wave is shifted upward, while the propagation constant of the sine wave is shifted downward, as shown in Fig. 2(b). For shallow gratings this shift is proportional to the grating amplitude.[11] An alternative way to understand intuitively

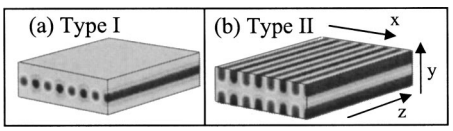

Fig. 1. Schematic index structure of (a) Type I (bell-shaped) and (b) Type II (trough-shaped) GMWs.

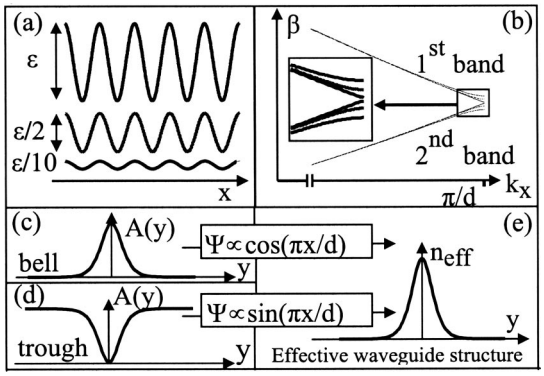

Fig. 2. (a) Index grating with three different amplitudes corresponding to three different y planes ("layers") in GMWs. (b) The dispersion curves (propagation constant β versus the transverse momentum k_x) near the edge of the first Brillouin zone for the gratings shown in (a). The inset shows the dispersion curves at the edge of the first Brillouin zone. Typical grating index amplitudes of (c) Type I and (d) Type II GMWs. (e) The effective waveguide structure in y; Type I beams need a $\cos(\pi x/d)$ dependence, Type II beams need a $\sin(\pi x/d)$ dependence to experience Bragg-mediated wave guiding.

these shifts at $k_x = \pm K_G/2$ is to view the standing waves as two propagating waves that propagate in angles $\pm\theta_{Bragg}$. The two Bragg-matched waves scatter into one another, that is, the wave propagating at angle θ is scattered and coherently added to the wave that is propagating at $-\theta$, and vice versa. However, if the intensity of the interference pattern between the two waves is in phase with the index grating, i.e., the intensity has a $\cos^2(K_G x/2)$ structure, then the scattered waves are $\pi/2$ *phase-delayed* relative to the waves into which they are scattered and to which they are coherently added.[5] Thus these multiple Bragg reflections between the two waves decrease the phase velocity (increasing the propagation constant and effective index) of both waves as a consequence of the interaction between the waves and the grating. In contrast if the intensity of the interference pattern is $\sin^2(K_G x/2)$, i.e., it is π phase-shifted relative to the index grating, then the scattered waves are $\pi/2$ *phase-advanced* relative to the waves into which they are scattered. Thus in this case their phase velocity is increased (their propagation constant and effective index are decreased).

The first type of GMW, Type I [see Fig. 1(a)], has a bell-shaped amplitude in y [Fig. 2(c)]. The change in propagation constant (the effective index) for the $\cos(\pi x/d)$ grating mode due to the presence of the grating is proportional to the grating amplitude $\varepsilon A(y)$. Hence beams with a $\cos(\pi x/d)$ dependence experience effective wave guiding in y, that is, the effective index for such beams has a waveguide structure as shown in Fig. 2(e).

GMW of the second kind, Type II [see Fig. 1(b)], relies on a trough-shaped grating amplitude $A(y)$ [Fig. 2(d)]. Here the change in propagation constant β (the effective index) for beams having a $\sin(\pi x/d)$ dependence is proportional to $-\varepsilon A(y)$, which (again) results in an effective waveguide structure for these sine beams [Fig. 2(e)].

3. COMPARISON WITH OTHER WAVE-GUIDING METHODS

It is instructive to highlight the difference between GMW and waveguides that rely either on Bragg reflection or on

TIR. At first sight, one might think that because the structures of GMWs are periodic, the wave guiding effect is identical to that of Bragg-reflection waveguides.[6–8] This view is misleading, and in fact the methods are different. Specifically, in Bragg-reflection waveguides the waves are Bragg-reflected from the cladding regions back into the core region, i.e., the reflections are in the plane defined by the propagation and confinement directions. In contrast, for a GMW the grating is perpendicular to the direction of confinement and the confined waves are Bragg-scattered in the direction normal to the confinement direction. Likewise, GMWs are different from TIR waveguides: In TIR structures the light is confined in regions of higher refractive index,[5] whereas for GMW all the waveguide "layers" have the same average refractive index n_0. This last argument becomes more apparent in Type II GMWs, for which the grating amplitude has a trough shape. In this case wave guiding is achieved even though light is not concentrated in the regions of the peaks of the refractive index. Another important difference between GMW and Bragg-reflection waveguides is that the former is both Bragg sensitive and phase sensitive, whereas the latter is sensitive only to Bragg mismatch. That is, for GMWs the actual phase (and not just the periodic structure) of a wave determines whether a beam will be guided or deflected. This allows for sophisticated structures to be created, such as the GMW "superlattices" that will be discussed below.

4. FINDING THE GUIDED MODES OF A GRATING-MEDIATED WAVEGUIDE

We use coupled-mode theory to find the guided modes of the GMW. Since the index change is very small we neglect any vectorial effects, assume quasi-monochromatic light, and solve for the guided modes $\Psi_\beta(x,y)$ and propagation constants β of the scalar Helmholtz equation

$$\frac{\partial^2\Psi}{\partial x^2}+\frac{\partial^2\Psi}{\partial y^2}+(k_0{}^2n^2-\beta^2)\Psi=0, \tag{2}$$

where $n(x,y)$ is given by Eq. (1) and $k_0=\omega/c$. Following our principles we seek modes of the form $\Psi(x,y)=\Phi(y)\times\begin{bmatrix}\cos(\pi x/d)\\ \sin(\pi x/d)\end{bmatrix}$. Inserting this ansatz and Eq. (1) into Eq. (2) and neglecting terms of order ε^2 yields

$$\begin{bmatrix}\cos(\pi x/d)\\ \sin(\pi x/d)\end{bmatrix}\{\Phi''+\Phi[k_0{}^2n_0{}^2-(\pi/d)^2-\beta^2 + 2\varepsilon A(y)k_0{}^2n_0{}^2\cos(2\pi x/d)]\}=0. \tag{3}$$

Using trigonometric identities and neglecting asynchronous terms of spatial frequency $3\pi/d$, we obtain

$$\Phi''+\Phi[k_0{}^2n_0{}^2-(\pi/d)^2-\beta^2\pm\varepsilon k_0{}^2n_0{}^2A(y)]=0, \tag{4}$$

where the plus and minus signs correspond to the $\cos x$ and $\sin x$ dependences of $\Psi(x,y)$, respectively.[12]

Consider first Eq. (4) with the plus sign. As a concrete example of a Type I waveguide, we analyze the case where $A(y)=\mathrm{sech}^2(y/y_0)$ with $y_0=(2/\varepsilon k_0{}^2n_0{}^2)^{1/2}$. The first guided (bound) solution to Eq. (4) is $\Phi_1=\mathrm{sech}(y/y_0)$ with propagation constant $\beta_1=[k_0{}^2n_0{}^2(1+\varepsilon/2)-(\pi/d)^2]^{1/2}$. The second guided mode is $\Phi_2=\tanh(y/y_0)$ with $\beta_2=[k_0{}^2n_0{}^2-(\pi/d)^2]^{1/2}$. We solved Eq. (2) numerically with the parameters $\varepsilon=10^{-4}$, $d=5$ μm, $k_0=2\pi$ μm^{-1}, and $n_0=2$ (resulting in $y_0\approx11.25$ μm), and find that the numerical solutions almost perfectly match the analytical solutions. The analytic approximation is excellent for shallow gratings with envelopes that are several times wider than the grating period. We emphasize, however, that the idea of GMWs works well beyond the regime described by coupled-mode theory.

To study GMW further we simulate the propagation of various beam configurations when launched into this system. Our simulation is carried out by a standard beam-propagation method (BPM) and is based on the paraxial version[5] of the Helmholtz equation. The parameters used are the same as in the previous paragraph. Figures 3(a)–3(c) show a typical evolution of such beams when they are not Bragg-matched with the index grating. Specifically, these figures show the evolution of a $\mathrm{sech}(y/y_0)$ beam launched on-axis. The beam broadens from 20 μm at $z=0$ to 150 μm at $z=2$ cm. In a homogenous medium with $n=n_0$ the same beam would have diffracted (broadened) to 167 μm. On the other hand Figs. 3(d)–3(f) display the evolution of a beam with the same shape in y but with a $\cos(\pi x/d)$ modulation in x. Such a beam displays stationary evolution, maintaining its narrow 20 μm width in y and thereby demonstrating GMW. However, as discussed above Type I GMW necessitates matching between the phase front of the propagating field and the grating. This phase selectivity is demonstrated in Figs. 3(g)–3(i), which show the evolution of a single $\mathrm{sech}(y/y_0)$ beam that is incident at the Bragg angle and that can also be viewed as a superposition of a $\cos(\pi x/d)$ and a $\sin(\pi x/d)$ beam. As shown, the sine component radiates [Fig. 3(h)], whereas the cosine component stays guided within the structure.

Next we demonstrate Type II GMW, that is, when the grating envelope in y has a trough shape. We solve Eq. (4)

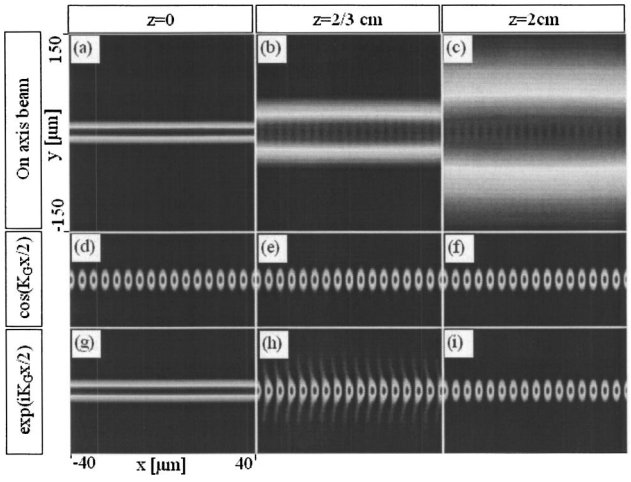

Fig. 3. Propagation of different beams in a Type I (bell-shaped) GMW, each with a y profile of the first guided mode. Shown are the intensities at the propagation planes $z=$(a) 0, (b) 2/3 cm, and (c) 2 cm for a beam uniform in x, (d)–(f) a beam with $\cos(\pi x/d)$ dependence, and (g)–(i) a beam with $\exp(i\pi x/d)$ dependence. Note that for the exponential profile, the sine component radiates while the cosine component is trapped.

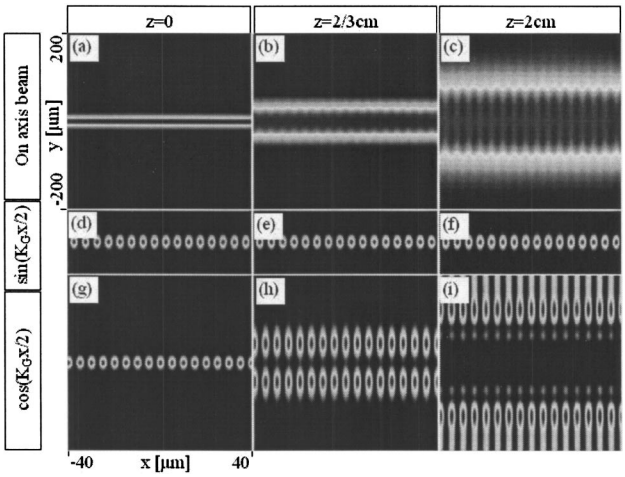

Fig. 4. Propagation of different beams in a Type II (trough-shaped) GMW, each with a y profile of the first guided mode. Shown are the intensities at the propagation planes $z=$(a) 0, (b) 2/3 cm, and (c) 2 cm for a beam uniform in x (d)–(f), a beam with $\sin(\pi x/d)$ dependence, and (g)–(i) a beam with $\cos(\pi x/d)$ dependence.

with the minus sign and set $A(y)=1-\mathrm{sech}^2(y/y_0)$. The only difference in Eq. (4) in this example from the previous one is the constant term $\varepsilon k_0{}^2 n_0{}^2$. Hence the envelopes of the guided modes are identical to those of the previous example, $\Phi_1=\mathrm{sech}(y/y_0)$ and $\Phi_2=\tanh(y/y_0)$, but with different propagation constants: $\beta_1=[k_0{}^2 n_0{}^2(1-\varepsilon/2)-(\pi/d)^2]^{1/2}$ and $\beta_2=[k_0{}^2 n_0{}^2(1-\varepsilon)-(\pi/d)^2]^{1/2}$, respectively. Figure 4 shows the propagation dynamics in such a waveguide with the same parameters (ε,d,k_0,n_0) as in Fig. 3. Figures 4(a)–4(c) show the propagation of an on-axis $\mathrm{sech}(y/y_0)$ beam with a uniform x structure that broadens from 20 μm at $z=0$ to 190 μm at $z=2$ cm. Figures 4(d)–4(f) display the stationary evolution of the $\mathrm{sech}(y/y_0)\sin(\pi x/d)$ beam. On the other hand a beam that is $\mathrm{sech}(y/y_0)$ in y but has a $\cos(\pi x/d)$ shape in x broadens considerably [Figs. 4(g)–4(i)]. We emphasize that GMW occurs in this trough-shaped Type II structure in spite of the depression in the grating amplitude. Wave guiding, however, is achieved only at the proper angles of incidence and with the proper relative phase between the waves so that the interference maxima coincide with the valleys in the index grating.

The two envelopes (grating amplitudes) defining the bell and trough shapes are not the only envelopes allowing for GMW. It is also possible to create grating amplitudes $A(y)$ that arise from combinations of the two (bell and trough) cases. For example the structure with envelope $A(y)=\mathrm{sech}^2(y/y_0)-\tanh^2(y/y_0)$ also acts as a GMW in the vicinity of $y=0$. Another interesting example is $A(y)=\mathrm{sech}^2(y/y_0)-\tanh^2(y/y_0)\exp[-(y/4y_0)^2]$, which guides both the cosine and the sine beam components, but at different layers (in the vicinity, of $y=0$ and $y=\pm 2y_0$, respectively). A third example, called GMW superlattice will be discussed in Section 7.

5. EXPERIMENTAL PROOF OF CONCEPT

We now present an experimental proof of concept for GMW for both types, bell and trough. For the trough case, we generate the waveguide in a 5 mm long photorefractive SBN:60 crystal through optical induction. The waveguide is formed by interfering two plane waves that induce an index grating in the crystal. The trough is induced by illuminating the central interference region with a narrow stripe beam that is made incoherent with the interfering waves. The stripe beam acts to "bleach" the grating by reducing the visibility of the interference in the region of the stripe.

Together these three beams induce, through photorefractive diffusion effects (with no external field applied and with no apparent photovoltaic effect), a trough-type GMW structure [Fig. 5(a)] of[5]

$$\Delta n \propto I_1 \cos(2\pi x/d+\pi/2)/[I_1+I_2\exp(-y^2/y_0{}^2)].$$

Here d is the periodicity of the grating-intensity interference pattern, y_0 the width of the stripe, and I_1, I_2 the peak intensities of the grating and stripe beams, respectively. The beams inducing the waveguide are ordinarily polarized, for which the electro-optic coefficient in SBN:60 is negligibly small. Hence the waves inducing the grating experience approximately linear propagation and no energy exchange (two-wave mixing), as if they were propagating in a homogeneous linear medium.

Next we launch the probe beams into the trough structure. The probe beams are made very weak so as not to affect the waveguide structure. At the same time, the probe beams are extraordinarily polarized; hence they "feel" the waveguide structure through the large electro-optic coefficient. To generate a probe beam with a proper guided-mode profile, we interfere two beams that are wide in x, narrow in y, propagating at $\pm\theta_{Bragg}$ with respect to the z axis, and possesing the "correct" π phase shift relative to the grating index. Figures 5(b) and 5(c) show the intensity pattern at the input and output faces of the crystal, respectively, demonstrating the confinement of the beam in the GMW structure. For comparison Figs. 5(d)–5(f) show diffraction in three different conditions: propagation in a homogeneous medium [Fig. 5(d)], when the beams are not Bragg-matched with the index grating [Fig. 5(e)], and when the beams are Bragg-matched with

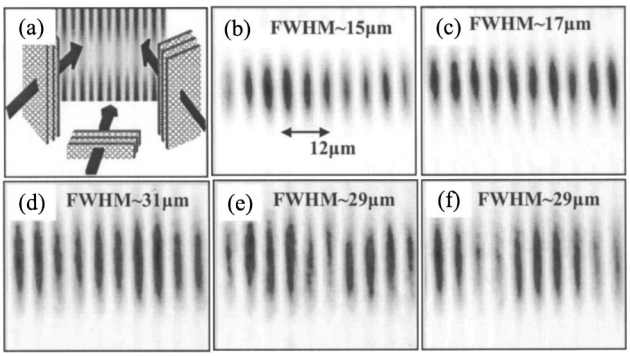

Fig. 5. (a) Schematic of the optically-induced technique we use to obtain a Type II GMW. Photographs of a probe beam at the (b) input and (c) output of the waveguide providing experimental proof of concept for GMW. Diffraction in unguided conditions: (d) a homogeneous medium, (e) when the beams are not Bragg-matched with the index grating, (f) when the beams are Bragg-matched with the grating but have the "wrong" phase relative to the grating. In (b)–(f) the intensity in each figure is normalized to its own peak intensity.

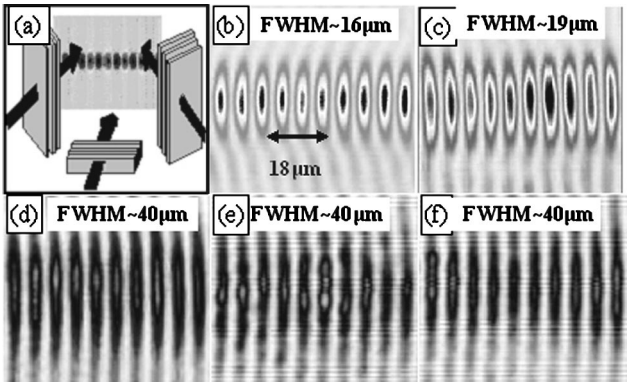

Fig. 6. Same as Fig. 5 but for a Type I GMW.

the grating but have the "wrong" phase relative to the grating [Fig. 5(f)]. Clearly the probe beam is guided in the GMW structure under the proper periodicity and phase conditions.

For the case of a bell-type GMW we use a similar technique as with the trough, this time with a 7 mm long photorefractive SBN:60 crystal. We can use a longer crystal because of the way we induce the bell-shaped structure. Instead of the bright stripe of light that was used for the trough-shaped GMW to "bleach" the central region of the grating and thereby induce the trough envelope, we now need to bleach the other regions of the grating (in the y direction). We therefore need to bleach the grating with a dark stripe beam. We generate such a bleaching beam by use of the reflection from a step mirror fabricated by photolithography. This mirror has a $\lambda/4$ step in its middle, causing a π phase shift and resulting in a dark stripe across the middle of the beam. This beam superimposed on the interference bleaches the grating everywhere except in the middle region (the region of the dark stripe) thereby inducing a bell-type GMW structure[5] [Fig. 6(a)] of

$$\Delta n \propto I_1 \cos(2\pi x/d + \pi/2)/[I_1 + I_2 \tanh^2(-y^2/{y_0}^2)].$$

Again, we launch the probe beams into the bell-shaped GMW structure. Figures 6(b) and 6(c) show the intensity pattern at the input and output faces of the crystal, respectively, demonstrating the confinement of the beam in the bell structure. For comparison Figs. 6(d)–6(f) show diffraction in three different conditions: propagation in a homogeneous medium [Fig. 6(d)], when the beams are not Bragg-matched with the index grating [Fig. 6(e)], and when the beams are Bragg-matched with the grating but have the "wrong" phase relative to the grating. Once again the probe beam is guided in the GMW structure under the proper periodicity and phase conditions.

Comparing the trough-shaped and the bell-shaped GMWs, both generated through optical induction, we find that the optically induced bell structure can be made to extend over larger distances (7 mm long versus 5 mm long for the trough shape) for a waveguide of the same width. The limitation on the propagation length within such a waveguide is *not* fundamental to GMW, but rather arises from the optical induction technique. Basically, the stripe beam used in inducing the trough-shaped GMW is propagating linearly in the photorefractive crystal, thus experiencing diffraction broadening. The largest distance over which the diffraction of the stripe beam is negligible determines the largest propagation distance in such an optically-induced trough GMW. The bell-shaped GMW, on the other hand, is induced with a beam possessing a dark stripe in the middle. The step mirror we use creates an antisymmetric beam whose central dark region experiences less diffraction broadening than the bright stripe of the same width. That being said, fundamentally, for GMWs generated using fabrication techniques, the two types of waveguide structure should be fully equivalent.

6. GUIDED MODES WITH DETUNING

In trying to establish the robustness of the new GMW method, we simulate its behavior under detuning from the Bragg condition. That is, we study how well a beam can be guided in a GMW when the beam is not perfectly Bragg-matched with the waveguide grating. There are two types of deviations form Bragg-matching (detuning along the x axis). The first is the variation of the angle between the probe beams by an amount 2δ such that the grating wave number (periodicity) of the probe changes [Fig. 7(a)]. The second type of detuning is the variation of the angle between the probe interference structure and the waveguide grating by an amount Δ while keeping the angle between the probe beams 2θ unchanged [Fig. 7(b)]. This second type of detuning means essentially rotating both probe beams together in the same direction so that their interference wave number remains equal to that of the GMW, but the directions of the respective wave vectors are no longer parallel. In the first case (which we simulated but do not show here) the GMW structure displays very little tolerance, as expected from Bragg detuning. This is actually a positive feature, since the GMW filtering capability is based on high phase sensitivity for the probe. For the second case our numerical simulations show that there is a region of robustness of the GMW system that allows for some misalignment between the directions of the corresponding wave vectors. This robustness is essential if GMWs are to be used in real applications.

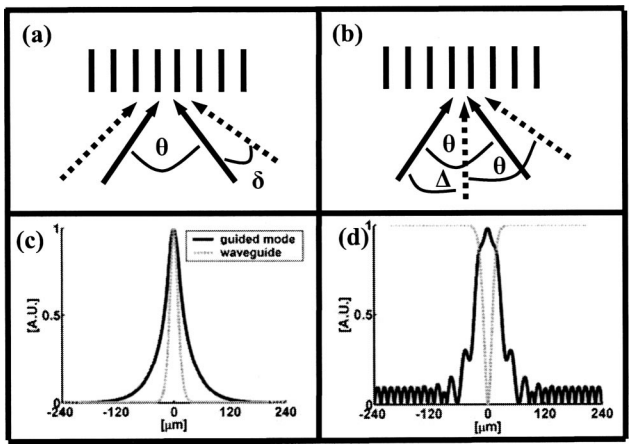

Fig. 7. Detuning in x direction of a probe entering a GMW. (a) Shifting of each beam by an equal opposite angle δ, (b) shifting both beams together by an angle Δ in one direction relative to the waveguide grating. Numerical results showing the guided modes for (c) Type I and (d) Type II GMW with detuning of 2.5%, both for a type of detuning described in (b).

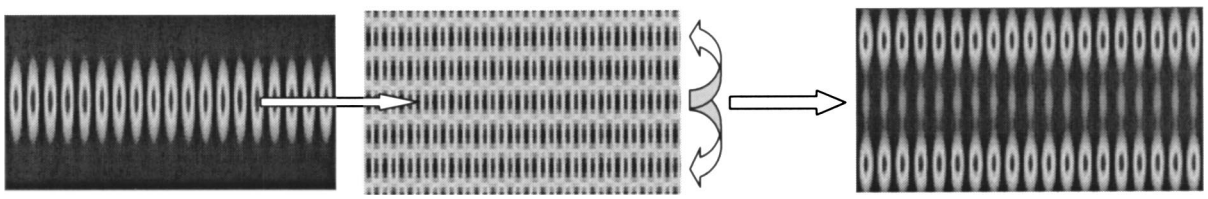

Fig. 8. Discrete diffraction in a simulated 2D GMW superlattice. The phase of the probe itself relative to the initial superlattice layer determines whether that particular layer of the superlattice will act as a waveguide.

Figures 7(c) and 7(d) show typical results from our numerical calculations for bell-shaped and trough-shaped GMWs, respectively, where the guided modes are calculated under detuning of 2.5% from perfect alignment. That is, we calculate the eigenmodes of the structure for a propagation direction that is tilted by $\approx 0.14°$ with respect to z, and then calculate the modal confinement factors as the overlap integral of the modal field with the absolute value of the waveguide envelope in the y direction. In so doing we define (arbitrarily) a guided (localized) mode if its confinement factor exceeds 60%. Under these conditions the maximum level of detuning in this system that still supports a localized mode is $\approx 3.5\%$ of the transverse wave vector k_x for the bell shape and $\approx 3\%$ of the transverse wave vector k_x for the trough shape. This measure of detuning in the wave vector corresponds to $\approx 0.2°$ of detuning in the incidence angle of the probe beams.

7. FUTURE RESEARCH AND APPLICATIONS

After analyzing in detail the 1D GMW structure, we can start to look at more complex GMW structures in 2D. One idea that comes to mind is the 2D GMW "ring," whose guided modes are periodically modulated 2D light rings. Such 2D structures can be thought of as folded 1D bell–trough-shaped GMWs. These GMW shapes can be used as sensitive phase filters for ring beams by taking advantage of their high Bragg and phase selectivity to guide beams with the proper topological charge and proper phase.

Another idea is the GMW "superlattice" (see Fig. 8). This structure has a periodic amplitude not only in x but also in y such that $A(y)=\cos(y/y_0)$, which results in an array of bell-shaped GMWs with a π phase shift between them. In this generic structure, beams with different x dependences experience different "effective structures" in y. Specifically, beams with $\cos(\pi x/d)$ exhibit wave guiding in layers $y=2\pi y_0 m$, whereas beams with $\sin(\pi x/d)$ are guided at $y=\pi y_0(1+2m)$ (where $m=0,\pm 1,\pm 2\ldots$). At the same time beams lacking spatial frequency of π/d do not "feel" any waveguiding effects but behave approximately as they would in a homogenous medium. In this unique structure the probe beams themselves determine where they will be guided, according to their phase. In Fig. 8 we show that a probe beam under normal incidence propagation in the superlattice undergoes "discrete diffraction"[13,14] in y, in a fashion similar to waves propagating in photonic lattices.[15–17] It will be particularly interesting to study discrete diffraction and lattice solitons[18–21] in these special structures.

A holographic soliton,[22] which is a soliton supported solely by holographic focusing, is another very interesting structure related to GMWs, although such solitons are of course inherently *nonlinear* entities. In fact a holographic soliton can be thought of as a self-induced GMW. When a waveguide is induced by the same light beam guided in it, the beam is a soliton. If the beams guided in a GMW are the waves creating–inducing it, the jointly trapped beams form a so-called holographic soliton: a self-trapped entity that forms by virtue of Bragg reflection of two waves into one another from a grating that these waves jointly induce. When these simultaneous Bragg reflections are properly phase-delayed, a bright (or dark) holographic soliton forms.[22] Unlike all other kind of solitons, holographic solitons are supported solely by XPM due to reflections from the induced grating and not involving self-phase modulation at all. Holographic solitons have not been observed experimentally yet, although evidence for grating-induced self-focusing–defocusing has already been reported.[23]

Throughout this paper we have considered grating-mediated wave guiding in the optical domain. However, the GMW mechanism is generic and clearly applicable to any (2+1)D or (3+1)D wave system, i.e., any system that can be represented by the Helmholtz equation [Eq. (2)], the Schrödinger equation, or closely related equations. For example a periodic density variation with a transverse envelope profile (established, say, by a standing wave of suitable frequency) can guide acoustic or ultrasonic waves. The only requirement is the ability to create (or induce) a sinusoidal grating and propagate in the structure a distance greater than the grating period by orders of magnitude. This can be readily achieved with sound waves,[24] as well as with matter waves.[25] Indeed, any coherent wave propagating in a potential that is periodic in one dimension with a slowly varying amplitude in one or two transverse dimensions will experience Bragg-mediated wave guiding.

8. SUMMARY AND CONCLUSIONS

In conclusion we have presented a comprehensive study providing additional experimental and theoretical results of the new method of optical wave guiding, the so-called grating-mediated wave guiding. This wave-guiding method is driven by a shallow 1D grating with a bell-or trough-shaped amplitude that is slowly varying in the direction normal to the grating wave vector. This wave-guiding method can support new structures such as the GMW superlattice and GMW ring, and is also applicable to matter waves, acoustic waves, and other wave systems in nature in which a polarization grating can be generated.

ACKNOWLEDGMENTS

This work was supported by the Binational USA-Israel Science Foundation, the Israeli Science Foundation, and by the German-Israeli DIP project.

REFERENCES

1. G. P. Agrawal, *Fiber-Optic Communication Systems*, 2nd ed. (Wiley, 1997).
2. V. I. Kopp, V. M. Churikov, J. Singer, N. Chao, D. Neugroschl, and A. Z. Genack, "Chiral fiber gratings," Science **305**, 74–75 (2004).
3. J. C. Knight, J. Broeng, T. A. Birks, and P. St. J. Russell, "Photonic band gap guidance in optical fibers," Science **282**, 1476–1478 (1998).
4. D. Collodon and J. Babinet, Comptes Rendes **15**, 800 (1842).
5. A. Yariv, *Optical Electronics in Modern Communications* (Oxford, 1997).
6. P. Yeh and A. Yariv, "Bragg reflection waveguides," Opt. Commun. **19**, 427–430 (1976).
7. M. Ibanescu, Y. Fink, S. Fan, E. L. Thomas, and J. D. Joannopoulos, "An all-dielectric coaxial waveguide," Science **289**, 415–419 (2000).
8. P. St. J. Russell, "Photonic crystal fibers," Science **299**, 358–362 (2003).
9. A. Yariv, Y. Xu, R. K. Lee, and A. Scherer, "Coupled-resonator optical waveguide: a proposal and analysis," Opt. Lett. **24**, 711–713 (1999).
10. O. Cohen, B. Freedman, J. W. Fleischer, M. Segev, and D. N. Christodoulides, "Grating-mediated waveguiding," Phys. Rev. Lett. **93**, 103902 (2004).
11. N. W. Ashcroft and N. D. Mermin, *Solid State Physics*, (Saunders, 1976).
12. In general, the grating modes at the edge of the first Brillouin zone that belong to the odd bands can be written as an infinite sum $\Sigma_{m=0}^{\infty} a_m \cos[(2m+1)\pi x/d]$. Here the grating is shallow; hence we neglect the coupling to higher bands and approximate the grating mode of the first band as $\cos(\pi x/d)$.[11] Similarly, we approximate the grating mode of the second band at the edge of the Brillouin zone as $\sin(\pi x/d)$.
13. A. L. Jones, "Coupling of optical fibers and scattering in fibers," J. Opt. Soc. Am. **55**, 261–271 (1965).
14. S. Somekh, E. Garmire, A. Yariv, H. L. Garvin, and R. G. Hunsperger, "Channel optical waveguide directional couplers," Appl. Phys. Lett. **22**, 46–48 (1973).
15. H. Eisenberg, Y. Silberberg, R. Morandotti, and J. Aitchison, "Diffraction management," Phys. Rev. Lett. **85**, 1863–1866 (2000).
16. M. J. Ablowitz and Z. H. Musslimani, "Discrete diffraction managed spatial solitons," Phys. Rev. Lett. **87**, 254102 (2001).
17. Y. V. Kartashov, V. A. Vysloukh, and L. Torner, "Rotary solitons in Bessel optical lattices," Phys. Rev. Lett. **93**, 093940 (2004).
18. D. N. Christodoulides and R. I. Joseph, "Discrete self-focusing in nonlinear arrays of coupled waveguides," Opt. Lett. **13**, 794–796 (1988).
19. D. N. Christodoulides, F. Lederer, and Y. Silberberg, "Discretizing light behavior in linear and nonlinear waveguide lattices," Nature **424**, 817–823 (2003).
20. H. Eisenberg, Y. Silberberg, R. Morandotti, A. Boyd, and J. Aitchison, "Discrete spatial optical solitons in waveguide arrays," Phys. Rev. Lett. **81**, 3383–3386 (1998).
21. J. Fleischer, M. Segev, N. Efremidis, and D. N. Christodoulides, "Observation of two-dimensional discrete solitons in optically induced nonlinear photonic lattices," Nature **422**, 147–150 (2003).
22. O. Cohen, T. Carmon, M. Segev, and S. Odoulov, "Holographic solitons," Opt. Lett. **27**, 2031–2033 (2002).
23. M. Vaupel, C. Seror, and R. Dykstra, "Self-focusing in photorefractive two-wave mixing," Opt. Lett. **22**, 1470–1472 (1997).
24. R. J. D. Miller, M. Pierre, T. S. Rose, and M. D. Fayer, "A coherent photoacoustic approach to excited-state–excited-state absorption spectroscopy: application to the investigation of a near-resonant contribution to ultrasonic diffraction," J. Phys. Chem. **88**, 3021–3025 (1984).
25. M. Greiner, O. Mandel, T. W. Hansch, and I. Bloch, "Collapse and revival of the matter wave field of a Bose–Einstein condensate," Nature **419**, 51–54 (2002).